Archives of Public Health

RESEARCH

Open Access

COVID-19 RT-qPCR-based screening in Austrian schools and incidences in the general population: a Bayesian spatiotemporal analysis

Yessika Adelwin Natalia[1*], Sereina Annik Herzog[2], Thomas Neyens[1,3], Christoph Johann Zurl[4], Volker Strenger[4], Geert Molenberghs[1,3] and Christel Faes[1]

Abstract

In 2021, the emergence of highly transmissible COVID-19 variants of concern increased susceptibility among younger populations. Despite this risk, face-to-face education remained essential for societal functioning and children's well-being, prompting the Austrian government to implement a nationwide screening program in educational institutions. This study explores the impact of this program on COVID-19 transmission by examining the relationship between incidence rates and factors such as age, vaccination coverage, and RT-qPCR positivity rates among school-aged children across Austrian districts, using a Bayesian spatiotemporal discrete model. Our findings highlight significant effects of vaccination and positivity rates on COVID-19 incidence, with variations in their influence across different age groups and locations. These results underscore the importance of monitoring these variables, particularly when active screening programs are in place.

Keywords Austria, COVID-19, RT-qPCR, Screening, School, Spatiotemporal analysis

*Correspondence:
Yessika Adelwin Natalia
yessikaadelwin.natalia@uhasselt.be
[1] I-Biostat, Data Science Institute, Hasselt University, Hasselt, Belgium
[2] Institute for Medical Informatics, Statistics and Documentation, Medical University of Graz, Graz, Austria
[3] I-Biostat, Leuven Biostatistics and Statistical Bioinformatics Centre, KU Leuven, Leuven, Belgium
[4] Department of Pediatrics and Adolescent Medicine, Medical University of Graz, Graz, Austria

Text box 1. Contributions to the literature

- Evidence on the effectiveness of active PCR-based COVID-19 screening programs remains limited, particularly in school settings.
- Our findings highlight the significant impact of vaccination coverage and positivity rates on COVID-19 incidence, with notable variations in their effects across different age groups and geographic locations.
- These results provide valuable insights for disease surveillance and can inform policymakers in optimizing public health strategies.

Introduction

The heavy burden of the COVID-19 pandemic in Europe started in January 2020 when the first cases were identified in France [1]. As of April 20, 2025, there were more than 281 million cases and 2.2 million deaths registered in the European region [2].

The first case of COVID-19 in Austria was identified in January 2020 which then quickly became an outbreak related to ski-resort areas [3]. Similar to other European countries, Austria experienced multiple waves that hit harder in the older age population. By the time that COVID-19 vaccination was available on the market in January 2021, the government started a vaccination campaign aimed first at this population [4]. Unfortunately, even with the plan to expand the vaccination coverage by including younger age population, Austria experienced a strong increase in the number of daily SARS-CoV-2 infections, hospitalizations, and eventually COVID-19-related deaths, in November 2021 [5].

Many COVID-19 outbreaks have been reported after school re-opening in 2020 [6]. With the emergence of highly transmissible variants of concern such as Delta or Omicron, the younger population became more susceptible for COVID-19 infections. On the other hand, face-to-face education at school plays an important role in the societal function and children's well-being. To facilitate proper functioning of schools, Austria implemented a nationwide screening program within its educational institutions. In January 2021, a nationwide screening program using antigen-based self tests was implemented for students, teachers and administrative employees [7]. In September 2021, the screening program was expanded to include weekly real-time reverse transcription-quantitative polymerase chain reaction (RT-qPCR) testing, offering a more sensitive diagnostic tool to complement the antigen-based tests.

Several studies have reported the potential advantages of antigen-based self-testing over RT-qPCR-based testing in Austria during the early months of 2021, despite their lower sensitivity – ranging from 7.4% to 61.7%, depending on the positive predictive value and target age group – and very high specificity (greater than 99%) [8, 9]. Nevertheless, RT-qPCR-based testing remains the established gold standard for diagnosing COVID-19 [10]. To date, no studies have reported the initial results of RT-qPCR-based testing in the context of this nationwide screening campaign. Therefore, this study aimed to assess whether RT-qPCR-based screening results – specifically, test positivity rates – are directly associated with reported COVID-19 incidence in the population, while accounting for age distribution and the ongoing vaccination campaign in year 2021. On top of this, spatial and temporal dependencies at a finer administrative unit are incorporated in our analysis using a Bayesian modeling framework.

The rest of this paper is organized as follows. In "Materials and methods" section, we describe the data and methodology used to analyze the collected data. In "Results" section, we present the results and finally, a discussion is provided in "Discussion" section.

Materials and methods

Data

Austria consists of nine federal states and 116 districts as shown in Fig. 1. The average district population in

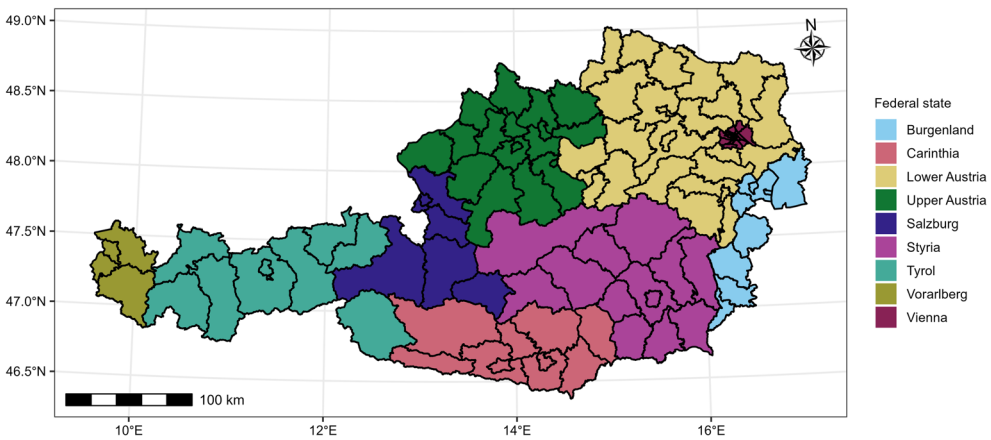

Fig. 1 Border of districts and federal states in Austria from September 13, 2021, to January 2, 2022

2021 was 77,006 inhabitants (range 2,000–291,134). We focused our analysis on school-aged children (6–18 years) which constituted around 12.4% of the total population.

The compulsory education in Austria is divided into three main school levels based on different age groups: primary school (grade 1–4, age 6–10 years), first secondary school (grade 5–8, age 11–14 years), and second secondary school (grade 9–12, age 15–18 years) [11]. Starting from January 2021, students were regularly tested for COVID-19 infection using anterior nasal swab antigen test. In September 2021, the testing scheme was expanded to include RT-qPCR test that analyzes multiple target genes. The implementation of the testing program varied slightly across federal states. In Burgenland, Upper Austria, Styria, and Vorarlberg, RT-qPCR testing was conducted every Monday, while antigen-based tests were administered twice weekly on Monday and Thursday. Meanwhile, in Carinthia, Lower Austria, Salzburg, and Tyrol, RT-qPCR testing took place on Tuesday, with antigen-based testing scheduled for Monday and Friday.

The screening results were documented by the Federal Ministry of Education, Science, and Research. The initiation of the RT-qPCR-based screening coincided with the start of the new academic year for compulsory education (beginning September 6 in Burgenland, Lower Austria, and Vienna, with other federal states starting later in the month). To ensure uniformity in the analysis, the study period was defined as September 13, 2021, to January 2, 2022 (weeks 37–52 according to ISO-8601). We excluded the federal state of Vienna from our analysis due to a different testing scheme within this region.

The vaccination campaign against COVID-19 was still ongoing in 2021. Therefore, we also retrieved data of vaccinated children in each district from the Austrian National Public Health Institute [12] to calculate the vaccination coverage within our study period. Data on COVID-19 incidences in the general population were provided by the Agency for Health and Food Safety [13]. The administrative map at district level and population data in 2021 per age category were made publicly available by Statistics Austria [14]. To ensure compatibility with the screening data, we excluded any population information from Vienna.

Statistical analysis

Exploratory data analysis

To provide a comprehensive overview of the collected data, we explored and visualized the temporal trends in weekly COVID-19 incidence, vaccination coverage, and positivity rates between September 13, 2021, and January 2, 2022. These trends were stratified by federal state and and three age groups (6–10 years, 11–14 years, and 15–18 years). We calculated the following variables:

1. COVID-19 incidence rate per 1,000 children, based on the registered place of residence.
2. Vaccination coverage, defined as the cumulative percentage of fully vaccinated children within each age group, also based on the registered place of residence.
3. Positivity rate from school-based screening, calculated as the number of positive tests per 100 tests conducted in the same federal state. To account for potential reporting delays, we used the sample collection date (i.e., the date the RT-qPCR test was performed) rather than the laboratory reporting date.

Univariate spatiotemporal model

For the following analysis, data were aggregated by district $i = 1, \ldots, 93$, defined either by school location or registered residence, over weekly periods $j = 1, \ldots, 16$ starting from September 13, 2021. The data were further stratified into three age groups $k = 1, \ldots, 3$ corresponding to age groups 6–10 years, 11–14 years, and 15–18 years, respectively.

Let O_{ijk} be the observed number of COVID-19 cases in district i during week j for age group k. Traditionally, count data are modeled using Poisson distribution, specified as:

$$O_{ijk}|\theta_{ijk} \sim \text{Poisson}(\mu_{\text{ijk}} = \text{N}_{\text{ijk}}\theta_{\text{ijk}}), \quad \log(\mu_{\text{ijk}}) = \log(\text{N}_{\text{ijk}}) + \log(\theta_{\text{ijk}}) \tag{1}$$

where μ_{ijk} denotes the mean (and variance) of the Poisson distribution, $N\ ijk$ refers to the population size, and θ_{ijk} represents the COVID-19 incidence rate [15].

Given the typically stringent assumptions of the Poisson model, it is important to allow for deviations. In general, count data may be overdispersed relative to the Poisson distribution, in the sense that the variance is larger than the mean. To accommodate this overdispersion, the Negative Binomial (NB) model is a popular choice, which can be denoted as:

$$O_{ijk}|\theta_{ijk} \sim \text{NB}(\text{r}, \mu_{\text{ijk}}) \tag{2}$$

where $r > 0$ is the size of overdispersion parameter relative to the Poisson model. The mean and variance of the distribution are defined as $\text{E}(\text{O}_{\text{ijk}}|\text{r}, \theta_{\text{ijk}}) = \mu_{\text{ijk}}$ and $\text{Var}(\text{O}_{\text{ijk}}|\text{r}, \theta_{\text{ijk}}) = \mu_{\text{ijk}}(1 + \frac{\mu_{\text{ijk}}}{\text{r}})$, respectively [16].

Further, the number of zero counts may be higher than expected under Poisson assumption, given the typically low incidence of COVID-19 among younger populations (the so-called zero-inflation). To take this into account, it is useful to consider the Zero-Inflated Poisson (ZIP) model, which accounts for both structural zeros (i.e., true

zeros that cannot be otherwise) and sample zeros (i.e., zeros arising by chance) [17]. Here, O_{ijk} is given by:

$$\begin{aligned} O_{ijk}|\theta_{ijk} &\sim \text{ZIP}(\mu_{\text{ijk}}, \pi_{\text{ijk}}) \\ P(O_{ijk}=0) &= \pi_{ijk} + (1-\pi_{ijk})\exp(-\mu_{ijk}), \qquad 0 \le \pi_{ijk} \le 1 \\ P(O_{ijk}=m) &= (1-\pi_{ijk})\frac{\mu_{ijk}^m \exp(-\mu_{ijk})}{m!}, \qquad m=1,\ldots,\infty, \qquad 0<\mu_{ijk}<\infty \end{aligned} \tag{3}$$

where π_{ijk} denotes the probability of a structural zero, while $1-\pi_{ijk}$ reflects the probability of a sample zero in district i, week j, and age group k.

Of course, it is entirely possible to encounter both overdispersion and excess zeros simultaneously [18], leading to the Zero-Inflated Negative Binomial (ZINB) model defined as:

$$\begin{aligned} O_{ijk}|\theta_{ijk} &\sim \text{ZINB}(\text{r}, \mu_{\text{ijk}}, \pi_{\text{ijk}}) \\ P(O_{ijk}=0) &= \pi_{ijk} + (1-\pi_{ijk})\left(\frac{r}{r+\mu_{ijk}}\right)^r \\ P(O_{ijk}=m) &= (1-\pi_{ijk})\binom{m+r-1}{m}\left(\frac{r}{r+\mu_{ijk}}\right)^r\left(\frac{\mu_{ijk}}{r+\mu_{ijk}}\right)^m \end{aligned} \tag{4}$$

When the overdispersion becomes very small ($r \to \infty$), the Negative Binomial component approaches a Poisson distribution, and the ZINB model converges to the ZIP model.

To account for the complex interplay between age groups, vaccination coverage, and COVID-19 test positivity rates, a three-way interaction term was included to model the joint effects of these explanatory variables. Since immunity requires time to develop following vaccination [19], we also explored lagged vaccination coverage as a potential explanatory variable. Specifically, we considered the impact of vaccination coverage lagged by l weeks, where $l = 0, 1, \ldots, 12$, corresponding to up to three months prior to the current week. This variable is denoted as $\text{vac}_{\text{i,j}-\text{l,k}}$, representing the vaccination coverage in district i, at week $j-l$, for age group k. Thus, for each likelihood, the incidence rate θ_{ijk} is modeled on the logarithmic scale as

$$\begin{aligned} \log(\theta_{\text{ijk}}) =& \beta_0 + \beta_{1k} + \beta_2 \text{vac}_{\text{i,j}-\text{l,k}} + \beta_3 \text{pos}_{\text{ijk}} + \beta_{4\text{k}} \cdot \text{vac}_{\text{i,j}-\text{l,k}} + \beta_{5\text{k}} \cdot \text{pos}_{\text{ijk}} \\ &+ \beta_6 \text{vac}_{\text{i,j}-\text{l,k}} \cdot \text{pos}_{\text{ijk}} + \beta_{7\text{k}} \cdot \text{vac}_{\text{i,j}-\text{l,k}} \cdot \text{pos}_{\text{ijk}} + \text{b}_\text{i} + \gamma_\text{j} + \delta_{\text{ij}}, \end{aligned} \tag{5}$$

The spatial random effect b_i is modeled using BYM2, a re-parametrization of the Besag-York-Mollie (BYM) model that incorporates penalized complexity (PC) priors [20, 21]. The scaled spatially structured component ν_{*i} and unstructured component υ_{*i} are defined as:

$$b_i = \frac{1}{\sqrt{\tau_b}}\left(\sqrt{1-\phi}\,\upsilon_{*i} + \sqrt{\phi}\,\nu_{*i}\right), \tag{6}$$

where τ_b denotes the marginal precision (inverse variance) parameter and ϕ denotes the mixing parameter that measures the proportion of the marginal variance explained by ν_{*i}.

For the temporally structured random effect γ_j, a random walk of order one (RW1) model denoted as $\gamma_j - \gamma_{j-1} \sim \text{N}(0, \tau_\gamma^{-1})$ is assumed [15]. Considering the dynamics between the spatial and temporal random effects, we included an independent and identically distributed (i.i.d.) interaction between spatially unstructured and temporally unstructured effects, i.e., $\delta_{ij} \sim \text{N}(0, \tau_\delta^{-1})$ [22].

To assess unusual elevations of COVID-19 incidence, we calculated the exceedance probability defined as the proportion of the incidence's posterior probability that exceeds a given threshold incidence value IR_0. The probability was calculated using the marginal posterior distribution of θ_{ijk}. In this study, we used the average of COVID-19 incidence as a threshold value. As suggested by Richardson et al., we classified areas where $P(\theta_{ijk} \ge \text{IR}_0) \ge 0.8$ as a hot spot, $P(\theta_{ijk} \ge \text{IR}_0) \le 0.2$ as a cold spot, and the other areas as statistically similar to the national average [23].

Model selection and prior sensitivity analysis

To identify the most appropriate likelihood function, an initial model without lagged vaccination coverage ($\text{vac}_{\text{i,j}-0,\text{k}}$) was fitted using the four candidate distributions (Poisson, NB, ZIP, and ZINB). Model performance was formally evaluated using several selection criteria: the Deviance Information Criterion (DIC) [24], the Watanabe-Akaike Information Criterion (WAIC) [25], the Conditional Predictive Ordinate (CPO), and the Probability Integral Transform (PIT) [26].

Both DIC and WAIC balance model fit and complexity, with lower values indicating better overall model performance.The CPO assesses the model's predictive ability for each observation, where higher individual CPO values suggest better predictive accuracy. In this study, a summary CPO statistic was calculated as the negative sum of the log-CPO values across all observations; smaller values of this summary measure indicate better

model fit [27]. The PIT evaluates the calibration of the model's predictive distributions: if the model adequately represents the observed data, the PIT values should follow a uniform distribution between 0 and 1. Deviations from uniformity (e.g., U-shaped or bell-shaped PIT histograms) may indicate model misspecification, overdispersion, or underdispersion.

After selecting the best-fitting likelihood, we fitted models incorporating various lagged vaccination coverage $\text{vac}_{i,j-l,k}$ and assessed their performance using DIC, WAIC, and the summary CPO metric.

The regression coefficients were given a normal prior distribution with zero mean and a small precision parameter of 0.001. As a sensitivity analysis for the spatial random effects, we fitted the proposed model with different values of user-defined upper bound U that specifies the tail event with weight α so that $P\left(\frac{1}{\sqrt{\tau_b}} > U\right) = \alpha$ (see Eq. 6). We defined four different U values: 0.5, 1, 2, and 5, with lower U values indicating more informative priors [21]. The mixing parameter was set to $P(\phi \leq 0.5) = 0.5$, meaning that the contribution of the structured and unstructured components is equal. The temporal random effect (RW1) and type I space-time interaction were first set to a default log-Gamma prior with parameters shape = 1 and inverse-scale = 0.00005. We then compared this default setting to a PC prior assuming $U = 1$ and $\alpha = 0.01$.

All analyses were performed in `R` version 4.4.1 [28]. The spatiotemporal models were fitted using `R-INLA` [29].

Results

Trend of COVID-19 positivity rates, incidences, and vaccination coverage

Between September 13, 2021, and January 2, 2022, a total of 130,529 COVID-19 cases were reported among school children with known residential information in Austria, in which 129,101 COVID-19 cases were located in our study area (Burgenland, Upper Austria, Styria, Vorarlberg, Carinthia, Lower Austria, Salzburg, and Tyrol). During the same period, 12,109,212 RT-qPCR test results were recorded from 5,637 schools across the country, including those located in Vienna. For our analysis, we excluded 2,725,279 test results from schools in Vienna as well as 47 tests associated with unknown school locations, resulting in a final dataset comprising 9,383,886 test results. Additionally, around 159,322 fully vaccinated children were registered.

Table 1 Model selection criteria for the initial model among school children in Austria, from September 13, 2021, to January 2, 2022. A lower value indicates a better model fit

Likelihood	DIC	WAIC	CPO
Poisson	27,841.73	29,177.67	14,704.98
NB	27,712.06	27,828.01	13,982.37
ZIP	27,847.37	29,178.87	14,703.26
ZINB	28,518.27	28,624.33	14,375.01

The weekly time trend of COVID-19 positivity rates, incidences, and vaccination coverage per federal state and age group are shown in Online Resource 1 (Figs. S1–S3). The positivity rate ranged from 0 to 1.01 per 100 tests, while the incidences ranged from 0.05 to 9.21 per 1,000 children. In certain federal states, the vaccination coverage by early 2022 reached 2.46% in the youngest age group, 5.85% in the 11–14 age group, and 5.3% in the oldest age group.

In Fig. S1, we noted a substantial increase in the COVID-19 positivity rates and incidences after the autumn holiday period between October 25 and November 3, 2021. Positivity rates increased similarly across all age groups and federal states, while the rise in COVID-19 incidences were less prominent in age group 15–18 years (Fig. S2). A considerable increase in the vaccination coverage was observed in age groups 11–14 years and 15–18 years for all federal states (Fig. S3).

Spatiotemporal analysis

The initial model with no lagged vaccination coverage under a NB likelihood demonstrated the best fit among the four candidate distributions, as this model yielded the lowest DIC, WAIC, and summary CPO values (Table 1). This result was further corroborated by the approximately uniform distribution of the PIT histogram shown in Fig. 2.

Model performance under different lagged vaccination coverage scenarios and prior specifications is summarized in Online Resource 2. Among the candidate models, the specification without lagged vaccination coverage ($l = 0$) yielded the lowest DIC, WAIC, and CPO values, compared to models with lagged vaccination coverage. Moreover, variations in prior specifications had minimal impact on these model selection criteria, suggesting the robustness of our proposed model. The final model, upon which the subsequent results are based, is specified as follows:

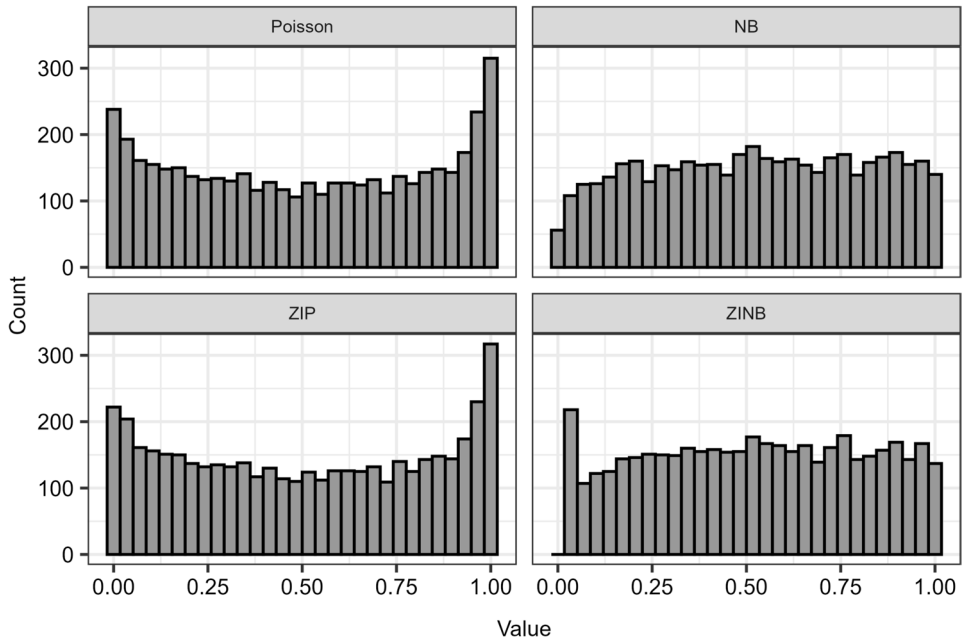

Fig. 2 Posterior predictive check based on PIT histogram for the initial model among school children in Austria, from September 13, 2021, to January 2, 2022

$$
\begin{aligned}
O_{ijk}|\theta_{ijk} &\sim \mathrm{NB}(\mathrm{r}, \mu_{\mathrm{ijk}}) \\
\log(\theta_{\mathrm{ijk}}) &= \beta_0 + \beta_{1\mathrm{k}} + \beta_2 \mathrm{vac}_{\mathrm{i,j-0,k}} + \beta_3 \mathrm{pos}_{\mathrm{ijk}} + \beta_{4\mathrm{k}} \cdot \mathrm{vac}_{\mathrm{i,j-0,k}} + \beta_{5\mathrm{k}} \cdot \mathrm{pos}_{\mathrm{ijk}} \\
&\quad + \beta_6 \mathrm{vac}_{\mathrm{i,j-0,k}} \cdot \mathrm{pos}_{\mathrm{ijk}} + \beta_{7\mathrm{k}} \cdot \mathrm{vac}_{\mathrm{i,j-0,k}} \cdot \mathrm{pos}_{\mathrm{ijk}} + \mathrm{b_i} + \gamma_{\mathrm{j}} + \delta_{\mathrm{ij}} \\
\beta_0, \beta_{1k}, \beta_2, \beta_3, \beta_{4k}, \beta_{5k}, \beta_6, \beta_{7k} &\sim \mathrm{N}(0, \tau_\beta^{-1}) \\
b_i &= \tfrac{1}{\sqrt{\tau_b}}\left(\sqrt{1-\phi}\, \upsilon_{*i} + \sqrt{\phi}\, \nu_{*i}\right) \\
\gamma_j - \gamma_{j-1} &\sim \mathrm{N}(0, \tau_\gamma^{-1}) \\
\delta_{ij} &\sim \mathrm{N}(0, \tau_\delta^{-1})
\end{aligned}
\tag{7}
$$

assuming default prior for each random effect, i.e. PC priors for the BYM2 model with $P\left(\frac{1}{\sqrt{\tau_b}} > 1\right) = 0.01$ and $P(\phi \leq 0.5) = 0.5$, while the RW1 and IID models were assigned log-Gamma priors.

Effect of age group, vaccination coverage, and positivity rate

The complete parameter estimates from the final model are presented in Table 2 (the corresponding posterior distributions are presented in Online Resource 1, Figs. S4 and S5). A statistically significant three-way interaction was identified between age group, vaccination coverage, and positivity rate, indicating that the relationship between positivity rate and COVID-19 incidence varies not only across age groups but also depending on the level of vaccination coverage. This complex interaction suggests that the effect of one variable cannot be interpreted independently of the others. The two-way interaction between vaccination coverage and positivity rate β_6 had a posterior mean of −0.008 (SD = 0.004), suggesting a modest negative interaction on the log scale. This implies that at higher positivity rates, the marginal effect of increased vaccination coverage on reducing COVID-19 incidence becomes slightly stronger, which translates to a greater decrease in incidence given the joint effect. However, this association is age-dependent. In the age group 6–10 years, the three-way interaction term β_{71} was positive (mean = 0.392, SD = 0.071), indicating a substantial attenuation or potential reversal of the vaccination benefit under high positivity rates. By contrast, the corresponding term in the age group 11–14 years had a mean near zero (0.002, SD = 0.006), implying no meaningful deviation from the average interaction pattern across all ages.

To better illustrate and interpret this interaction effect, we generated a dummy dataset comprising various combinations of vaccination coverage (ranging from 10% to 100%) and test positivity rates (ranging

Table 2 Parameter estimates for model based on Eq. 7 among school children in Austria, from September 13, 2021, to January 2, 2022

Variable	Parameter	Mean	SD	95% credible interval	
				Lower	Upper
Intercept	β_0	−4.505	0.086	−4.674	−4.336
Age group 6–10	β_{11}	−0.882	0.083	−1.045	−0.718
Age group 11–14	β_{12}	−0.541	0.075	−0.687	−0.395
Vaccination	β_2	−0.018	0.002	−0.021	−0.015
Positivity	β_3	0.828	0.225	0.388	1.27
Age group 6–10 · vaccination	β_{41}	−0.009	0.005	−0.019	0.0003
Age group 11–14 · vaccination	β_{42}	0.006	0.002	0.002	0.009
Age group 6–10 · positivity	β_{51}	−0.037	0.23	−0.487	0.414
Age group 11–14 · positivity	β_{52}	0.015	0.238	−0.451	0.482
Vaccination · positivity	β_6	−0.008	0.004	−0.017	0.0003
Age group 6–10 · vaccination · positivity	β_{71}	0.392	0.071	0.254	0.531
Age group 11–14 · vaccination · positivity	β_{72}	0.002	0.006	−0.011	0.014
Size (1/overdispersion)	r	22.005	1.402	19.377	24.894
Precision for spatial effect	τ_b	30.556	7.038	19.027	46.581
Mixing parameter	ϕ	0.695	0.155	0.351	0.932
Precision for temporal effect	τ_γ	4.564	1.602	2.137	8.36
Precision for type I interaction	τ_δ	9.374	0.572	8.296	10.548

SD standard deviation

from 0.1% to 3%) based on the observed values in our analysis. Using the final model, we calculated the posterior predicted COVID-19 incidence for each combination, as presented in Fig. 3. For ease of interpretation, vaccination coverage was color-coded using a 50% threshold to distinguish between low and high coverage scenarios. This visualization highlights how predicted incidence rates vary depending on the interaction between vaccination coverage and test positivity rate.

In general, we observed an increasing trend of COVID-19 incidences with higher positivity rates. This increase was more prominent in the age group 6–10 years, where the high positive logarithmic values of COVID-19 incidence indicated a sharp rise. On the other hand, age groups 11–14 and 15–18 years exhibited only minimal increases, as reflected by negative logarithmic values. Additionally, the increase in COVID-19 incidence rates in the two older age groups was more substantial when vaccination coverage was lower, as reflected by the positioning of the yellow lines above the green lines. The separation between high and low values of vaccination coverage was more pronounced in the oldest age group compared to age group 11–14 years. In contrast to this finding, a higher

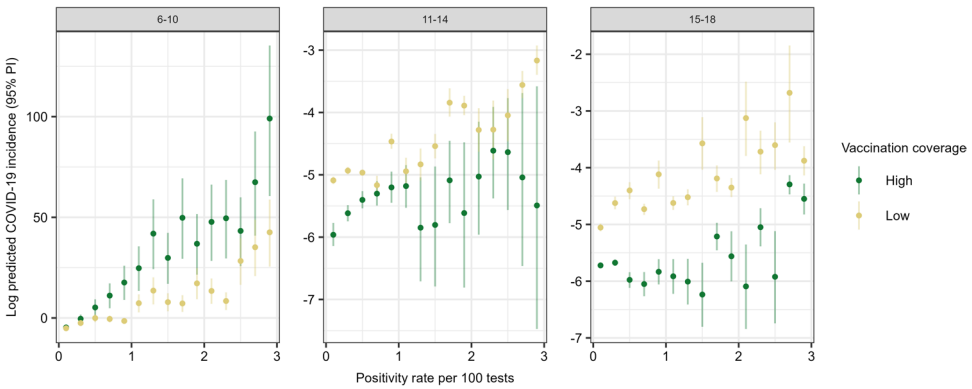

Fig. 3 Effect of age, vaccination coverage, and positivity rate on predicted COVID-19 incidence among school children in Austria, from September 13, 2021, to January 2, 2022. Green color indicates high vaccination coverage (≥ 50%) in the corresponding age group and yellow color indicates low vaccination coverage (< 50%). The *y*-axis range varies across age groups for clarity of the visualization. PI = predicted interval

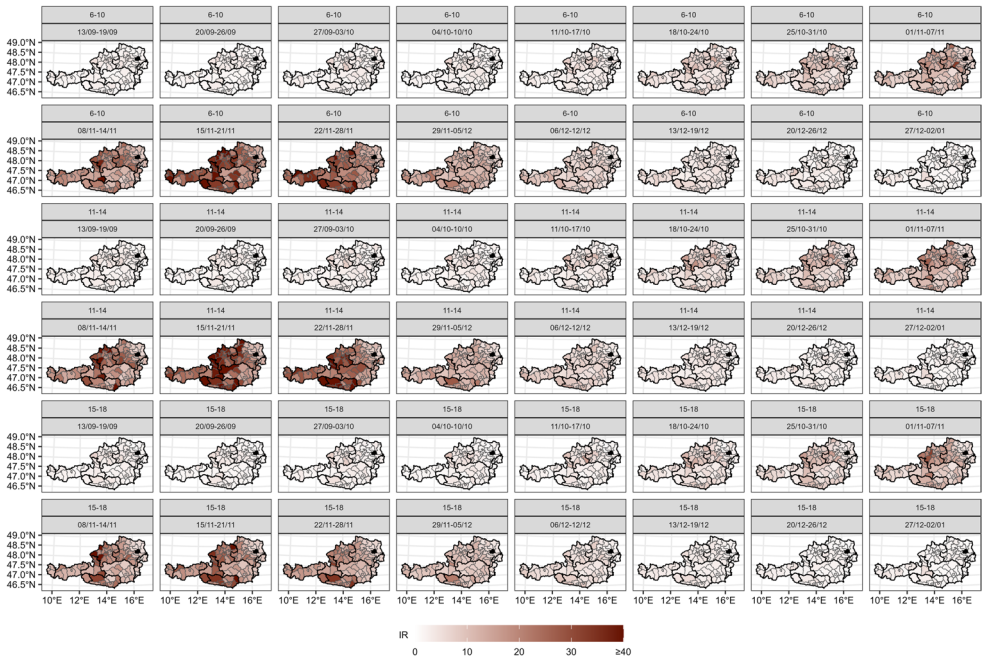

Fig. 4 Posterior COVID-19 incidence rate (IR) per 1,000 children at the district level in Austria, from September 13, 2021, to January 2, 2022. The border of each federal state is indicated with black lines. The federal state of Vienna, excluded from the analysis, is marked with black fill

COVID-19 incidence was observed despite higher vaccination coverage in age group 6–10 years, suggesting a different relationship between positivity rate, vaccination coverage, and COVID-19 incidence in this age group.

Mapping modeled COVID-19 incidences

The posterior COVID-19 incidences per district (excluding Vienna) are shown in Fig. 4. For all age groups, a notable increase in COVID-19 incidence was observed starting from the week of November 1–7, 2021, with peak incidences occurring between November 15 and November 28 in most municipalities, particularly in the regions of Carinthia, Lower Austria, Upper Austria, Salzburg, and Tyrol. The incidence then markedly decreased until it reached a similar level as during the first week of school by the start of January 2022.

To investigate the unusual COVID-19 incidence pattern, we calculated the exceedance probability with a threshold value of 20, as this value exceeds the average incidence across the entire study area and period. As illustrated in Fig. 5, the exceedance probability was markedly higher in Lower and Upper Austria starting in late October 2021. By week 45 (November 8–14, 2021),the majority of municipalities across the country could be classified as hot spots, before transitioning back to cold spots by the end of the study period.

To provide more insight, the weekly percentage of hot and cold spots by federal state and age group is illustrated in Fig. 6. A notable surge in the percentage of hot spot was observed across most federal states prior to the holiday period (particularly in Salzburg and Tyrol), with the exception of Burgenland. In Burgenland, the increase in hot spots occurred later and remained substantially lower compared to other federal states. Importantly, no hot spots were detected in the age group 15–18 years in Burgenland throughout the study period.

Discussion

This study identified a significant three-way interaction between age group, vaccination coverage, and test positivity rate in relation to COVID-19 incidence among school children in Austria. While the direction and magnitude of the fixed effects varied across the three age groups, indicating age-specific differences in how vaccination and community transmission interact, the underlying spatiotemporal patterns remained broadly consistent.

During the COVID-19 pandemic, schools have emerged as 'ideal' environments for viral transmission due to the relatively high frequency of social contacts (particularly in middle and high schools) and the prevalence of asymptomatic cases among younger individuals [30, 31]. In the exploratory analysis, we observed a similar temporal pattern between the positivity rate and

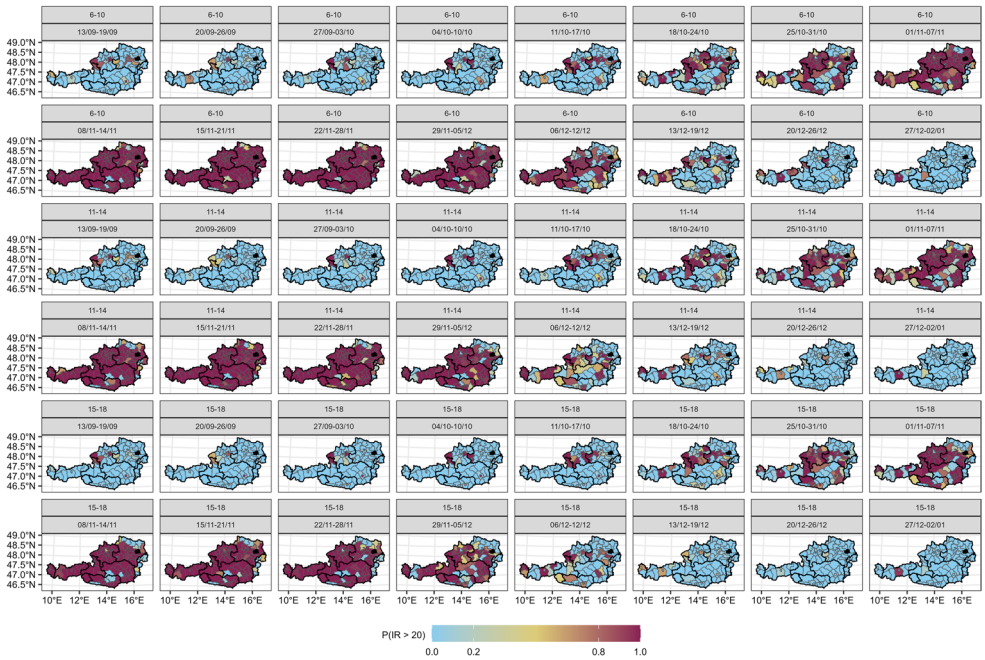

Fig. 5 Exceedance probability at the district level in Austria, from September 13, 2021, to January 2, 2022. IR = incidence rate per 1,000 children. The border of each federal state is indicated with black lines. The federal state of Vienna, excluded from the analysis, is marked with black fill

COVID-19 incidence (Figs. S1 and S2), highlighting a possible strong association between these indicators. This relationship is further substantiated in our spatiotemporal model, which revealed a consistent increase in COVID-19 incidence with higher positivity rates, after accounting for age group and vaccination coverage. Notably, the positivity rates observed in our study were relatively low, ranging from 0 to 1.01 per 100 tests at the federal state level and from 0 to 3.36 per 100 tests at the district level. Low positivity rate among school children

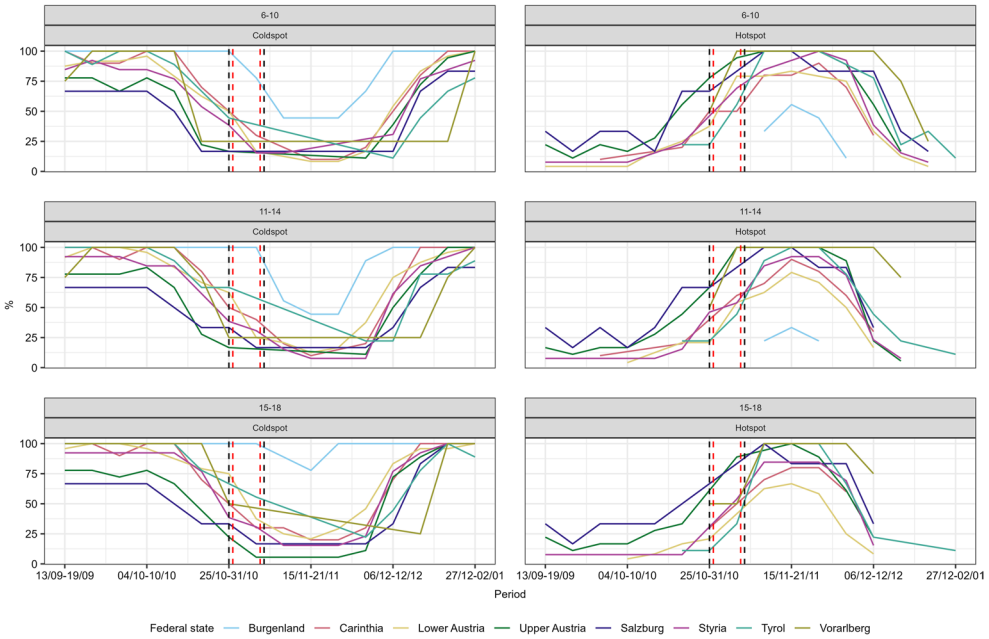

Fig. 6 Percentage of cold spots and hot spots in each federal state of Austria from September 13, 2021, to January 2, 2022. The holiday period in Burgenland, Upper Austria, Styria, and Vorarlberg is marked with red dashed lines. The holiday period in Carinthia, Lower Austria, Salzburg, and Tyrol is marked with black dashed lines

were also found in countries employing similar testing strategies such as Ireland [32], the United States [33], and Spain [34]. In contrast, other countries reported substantially higher positivity rates among children and adolescents, including Qatar [35] and Denmark [36].

Our findings are consistent with previous studies emphasizing the value of regular testing in school settings. Colosi et al. demonstrated that routine screening can effectively reduce SARS-CoV-2 transmission in schools while minimizing disruptions to education through reduced absenteeism [37]. Similarly, a study conducted in California found that weekly antigen testing with confirmatory RT-qPCR reduced transmission among students from kindergarten (typically ages 5–6) through grade 12 (ages 17–18), while limiting unnecessary absences due to false positives [38]. Both studies highlighted the importance of timing: national screening programs are most effective when population-level immunity remains low or during phases of moderate community transmission.

An important operational consideration is the delay between sample collection and result reporting, which can allow additional transmission from undetected positive cases [9]. To address this issue, we used the sample collection date rather than the laboratory reporting date, thereby improving the temporal alignment between exposure and case identification. Finally, although not the central focus of our study, we acknowledge the growing evidence that environmental factors such as air pollution and meteorological conditions may influence susceptibility to respiratory infections, including COVID-19 [39, 40].

Based on the estimated model parameter for the three-way interaction term β_{71} (mean = 0.392, SD = 0.071) and the posterior predicted values shown in Fig. 3, we observed an increasing trend in COVID-19 incidence with higher positivity rates in age group 6–10 years, even in the presence of higher vaccination coverage. This seemingly paradoxical pattern can be explained by the very low vaccination uptake in this age group during the study period. The European Medicines Agency (EMA) issued a recommendation for the use of the COVID-19 vaccine in children aged 5 to 11 on November 25, 2021 [41], which occurred relatively late in the timeline of our study.

In contrast, older school-aged children exhibited a more expected trend: higher vaccination coverage was associated with a milder increase in COVID-19 incidence, consistent with the protective effect of broader immunization. This effect was particularly evident in the age group 15–18 years, where a clear separation between low and high vaccination coverage scenarios was observed. Our findings likely reflect the substantially higher vaccination coverage in this age group compared to the younger age groups, highlighting the critical role of timely and widespread vaccination in school-aged children, on top of monitoring positivity rates, in mitigating COVID-19 infection, even with the emergence of new variants [42]. Of note, other possible factors related to age-specific behavioral or immunological differences, or variations in exposure patterns, should also be considered [43].

While these findings should be interpreted with caution due to the wide predictive intervals, they nonetheless underscore the potential consequences of delayed vaccine rollout on transmission dynamics among younger children. Moreover, it is important to recognize that the topic of COVID-19 vaccination in children continues to be a subject of ongoing debate, largely due to the balance between potential benefits and risks [44]. Additionally, many factors influence vaccination acceptance and behavior in the population. For instance, parents of fully immunized children are more likely to accept COVID-19 vaccination for their children, which then increased the COVID-19 vaccination coverage in the younger population [45].

In the early phases of the COVID-19 pandemic, children were considered to play a limited role in the transmission of SARS-CoV-2, as evidenced by lower reported case numbers and transmission rates among this age group in many countries [46]. However, this dynamic shifted notably with the emergence of more transmissible variants, such as Delta, which led to increased circulation of the virus within younger populations. In our study, a marked increase in COVID-19 incidence among school children was observed during the week of November 1–7, 2021, particularly in the federal states of Lower and Upper Austria (Fig. 4). This temporal pattern coincides with the widespread emergence of the Delta variant in Austria and its neighboring countries – including Czechia, Germany, and Slovakia – which also reported surges in pediatric COVID-19 cases during the same period [47].

Interestingly, localized hot spots of elevated COVID-19 incidence were already detectable at the beginning of the school year, with a notable concentration in urban areas (Fig. 5). These early signals suggest that schools in densely populated regions may have acted as focal points for transmission, potentially due to higher contact rates and mobility patterns. Similar trends were documented in Slovakia, where initial clusters of COVID-19 cases emerged in urban centers such as Bratislava and Košice before spreading to surrounding urban and rural districts. This resurgence, which occurred between June and August 2021, highlighted the vulnerability of children and adolescent to rapid changes in community transmission, particularly in the context of more transmissible variants and variable vaccination coverage [48]. Another

noteworthy spatiotemporal finding from our study is the consistently lower percentage of COVID-19 hot spots identified in Burgenland, with no hot spots detected at all in the age group 15–18 years throughout the entire study period. A plausible explanation for this pattern lies in the distinctly rural character of Burgenland, characterized by low population density and limited inter-district or cross-border mobility, which likely reduced opportunities for viral transmission within and between communities. Additionally, most districts in Burgenland achieved very high COVID-19 vaccination coverage among the general population in Austria during the study period, which may have contributed to lower infection rates through community-level immunity [12, 14].

The strength of our study lies in several aspects. First, using RT-qPCR data from schools provides a localized measure of viral prevalence to capture trends in transmission within a key demographic stratum. Second, the application of Bayesian spatiotemporal analysis enables us to account for both spatial and temporal dependencies in the data, providing more robust and reliable estimates of disease dynamics. Combining multiple nationwide data sources and advanced analytical techniques enhances the precision and relevance of our findings, contributing to more effective disease monitoring and response strategies. Finally, we acknowledge a minor difference in the spatial referencing of key variables: COVID-19 incidence and vaccination coverage were assigned according to the registered residence of the children, whereas positivity rates were linked to the location of the schools where testing was conducted. Rather than a limitation, we consider this distinction to be a methodological strength, as it allows the model to partially capture potential cross-district mobility, such as students commuting to schools outside their district of residence, which reflects real-world contact patterns more accurately. Incorporating this spatial heterogeneity may improve the explanatory power of the model and provide a more nuanced understanding of transmission dynamics across different geographic and social contexts.

Nevertheless, several limitations of this study should be acknowledged. There is a potential underestimation of positivity rates in the federal states of Carinthia, Lower Austria, Salzburg, and Tyrol due to the testing protocol employed. Children who tested positive using antigen-based tests on Monday were likely excluded from school attendance on Tuesday, the day RT-qPCR tests were conducted. However, we did not observe substantial differences in the total number of tests conducted and time trend of positivity rates (Fig. S1), suggesting that this potential bias may not have significantly impacted the overall findings. Furthermore, the integration of spatiotemporal effects in the analysis provides an additional layer of robustness, helping to address this limitation and ensuring a more comprehensive interpretation of the data.

On top of this, the use of district-level data may limit the granularity of our findings. Important variations in COVID-19 incidence rates likely exist at finer spatial scales, such as the municipality level, which could offer more detailed insights into localized outbreaks and transmission dynamics. By aggregating data at the district level, subtle within-district differences may be obscured, potentially underestimating the true spatial heterogeneity of COVID-19 infections. Lastly, our study did not include data on other non-pharmaceutical interventions (NPIs) such as social distancing measures, mandatory mask-wearing policies, travel restrictions, or active contact tracing efforts. These interventions may have an impact on COVID-19 transmission dynamics among school children [49], but their exclusion in our study was due to the lack of data at the district level. Moreover, we observed limited changes in the national stringency index during our study period [50]. When available, incorporating such data in future analyses could enhance the model's ability to assess the full range of factors affecting COVID-19 spread and provide a more comprehensive understanding of intervention effectiveness.

While our study offers valuable insights into the relationship between school-based testing, vaccination coverage, and COVID-19 incidence among children, it is important to acknowledge that the generalizability of our findings may be limited. Austria's national testing strategy – characterized by centralized, school-based RT-qPCR screening with high testing frequency – and its specific educational infrastructure (e.g., school size, attendance policies, and holiday schedules) may differ substantially from those in other countries. These contextual factors likely influenced both testing uptake and transmission dynamics, and thus, the observed associations may not fully translate to settings with different public health strategies, school systems, or population behaviors. Nonetheless, our findings underscore broader principles, such as the importance of early detection and timely vaccination, that can inform school-based mitigation policies globally. Future studies in diverse settings are warranted to evaluate how these findings hold under different epidemiological and policy contexts, and to identify adaptable strategies for reducing disease burden in school-aged populations.

Conclusion

Clearly, positivity rate and vaccination coverage had a significant impact on COVID-19 incidence in the younger population and the extent of their influence varies across

different age groups and locations. Therefore, it is crucial to monitor trends in these variables, particularly when active screening is feasible. Integrating multiple nationwide data sources with advanced analytical techniques offers valuable insights into disease dynamics over certain temporal and geographical contexts.

Supplementary Information

The online version contains supplementary material available at https://doi.org/10.1186/s13690-025-01655-8.

Additional file 1. Online Resource 1. Figs. S1 – S3: Time trend of COVID-19 positivity rates, incidences, and vaccination coverage stratified by age group and federal state. Figs. S4 – S5: Posterior distributions of the final model in Eq. 7.

Additional file 2. Online Resource 2. Summary of the model selection process based on Eq. 5.

Acknowledgements
The authors thank Gunter Maier from the Austrian National Public Health Institute for providing vaccination data used in this study. The authors also thank Patrick Pertl from the Federal Ministry of Education, Science, and Research for his critical input on the RT-qPCR-based screening data.

Authors' contributions
YAN participated in methodology, formal analysis, visualization, and writing the original draft. SAH contributed in study conception, data acquisition, interpretation of the results, and reviewing the manuscript. TN, GM, and CF involved in methodology, funding, and reviewing the manuscript. CJZ and VS were involved in data acquisition, interpretation of the results, and critical revision of the manuscript. All authors read and approved the final manuscript.

Funding
This research was supported by the BE-PIN project (TD/231/BE-PIN), funded by BELSPO (Belgian Science Policy Office) in the frame of the POST-COVID programme.

Data availability
The RT-qPCR data that support the findings of this study are available from the Federal Ministry of Education, Science, and Research, while the vaccination data were made available by the Austrian National Public Health Institute but restrictions apply to the availability of these data, which were used under license for the current study, and so are not publicly available. Data are however available from the authors upon reasonable request and with permission of the Federal Ministry of Education, Science, and Research, as well as the Austrian National Public Health Institute. Other datasets are publicly available.

Declarations

Ethics approval and consent to participate
Written informed consent to participate in the school screening program was obtained from the participants (children and/or their guardians). The Federal Ministry of Education, Science, and Research collected anonymized data as part of the program. For this study, only aggregated, anonymized RT-qPCR data were utilized, ensuring that no individual-level information was accessible. Consequently, ethical approval was not required for the analysis of these pre-existing anonymized data.

Consent for publication
Not applicable.

Competing interests
The authors declare no competing interests.

Received: 27 February 2025 Accepted: 8 June 2025
Published online: 13 June 2025

References

1. World Health Organization. Novel Coronavirus (2019-nCoV) situation report - 5, 25 January 2020. 2020. https://www.who.int/docs/default-source/coronaviruse/situation-reports/20200125-sitrep-5-2019-ncov.pdf?sfvrsn=429b143d_8. Accessed 15 Dec 2023.
2. World Health Organization. WHO Coronavirus (COVID-19) dashboard. 2024. https://covid19.who.int/. Accessed 6 May 2025.
3. Kreidl P, Schmid D, Maritschnik S, Richter L, Borena W, Genger JW, et al. Emergence of coronavirus disease 2019 (COVID-19) in Austria. Wien Klin Wochenschr. 2020;132(21–22):645–52. https://doi.org/10.1007/s00508-020-01723-9.
4. Pollak M, Kowarz N, Partheymüller J. Chronology of the Corona crisis in Austria - Part 4: Lockdowns, mass testing and the launch of the vaccination campaign. 2021. https://viecer.univie.ac.at/en/projects-and-cooperations/austrian-corona-panel-project/corona-blog/corona-blog-beitraege/blog100-en/. Accessed 18 Dec 2023.
5. Österreichische Agentur für Gesundheit und Ernährungssicherheit GmbH. Coronavirus. 2023. https://www.ages.at/mensch/krankheit/krankheitserreger-von-a-bis-z/coronavirus#c23235. Accessed 18 Dec 2023.
6. Hyde Z. COVID-19, children and schools: overlooked and at risk. Med J Aust. 2020;213(10):444-446.e1. https://doi.org/10.5694/mja2.50823.
7. Bundesministerium für Bildung, Wissenschaft und Forschung. Wissenschaftliche Begleitung zum Eintritts-Selbsttest (anterio-nasaler Antigen-Schnelltest) an österreichischen Schulen. 2023. https://www.bmbwf.gv.at/Themen/Forschung/Aktuelles/BeAntiGenT.html. Accessed 12 Feb 2024.
8. Willeit P, Bernar B, Zurl C, Al-Rawi M, Berghold A, Bernhard D, et al. Sensitivity and specificity of the antigen-based anterior nasal self-testing programme for detecting SARS-CoV-2 infection in schools, Austria, March 2021. Euro Surveill. 2021;26(34). https://doi.org/10.2807/1560-7917.Es.2021.26.34.2100797.
9. Polechová J, Johnson KD, Payne P, Crozier A, Beiglböck M, Plevka P, et al. SARS-CoV-2 rapid antigen tests provide benefits for epidemic control - observations from Austrian schools. J Clin Epidemiol. 2022;145:14–9. https://doi.org/10.1016/j.jclinepi.2022.01.002.
10. Corman VM, Landt O, Kaiser M, Molenkamp R, Meijer A, Chu DK, et al. Detection of 2019 novel coronavirus (2019-nCoV) by real-time RT-PCR. Eurosurveillance. 2020;25(3):2000045. https://doi.org/10.2807/1560-7917.ES.2020.25.3.2000045.
11. Bundesministerium für Bildung, Wissenschaft und Forschung. Die Schularten. 2024. https://www.bmbwf.gv.at/Themen/schule/schulsystem/sa.html. Accessed 12 Feb 2024.
12. Gesundheit Österreich GmbH. Gesundheit Österreich GmbH. 2024. https://goeg.at/. Accessed 12 Feb 2024.
13. Österreichische Agentur für Gesundheit und Ernährungssicherheit GmbH. Österreichische Agentur für Gesundheit und Ernährungssicherheit GmbH. 2024. https://www.ages.at/. Accessed 12 Feb 2024.
14. Statistik Austria. Statistics Austria Open.data. 2024. https://data.statistik.gv.at/. Accessed 12 Feb 2024.
15. Lawson AB. Using R for Bayesian spatial and spatio-temporal health modeling. CRC Press; 2021.
16. Gschlößl S, Czado C. Modelling count data with overdispersion and spatial effects. Stat Pap. 2008;49(3):531–52. https://doi.org/10.1007/s00362-006-0031-6.
17. Lambert D. Zero-inflated Poisson regression, with an application to defects in manufacturing. Technometrics. 1992;34(1):1–14.
18. Karim SA, Chen HF. Deaths from COVID-19 in rural, micropolitan, and metropolitan areas: a county-level comparison. J Rural Health. 2021;37(1):124–32. https://doi.org/10.1111/jrh.12533.
19. Li H, Wang L, Zhang M, Lu Y, Wang W. Effects of vaccination and non-pharmaceutical interventions and their lag times on the COVID-19 pandemic: Comparison of eight countries. PLoS Negl Trop Dis. 2022;16(1):e0010101. https://doi.org/10.1371/journal.pntd.0010101.

20. Riebler A, Sørbye SH, Simpson D, Rue H. An intuitive Bayesian spatial model for disease mapping that accounts for scaling. Stat Methods Med Res. 2016;25(4):1145–65. https://doi.org/10.1177/0962280216660421.
21. Daniel S, Håvard R, Andrea R, Thiago GM, Sigrunn HS. Penalising Model Component Complexity: A Principled, Practical Approach to Constructing Priors. Stat Sci. 2017;32(1):1–28. https://doi.org/10.1214/16-STS576.
22. Knorr-Held L. Bayesian modelling of inseparable space-time variation in disease risk. Stat Med. 2000;19(17–18):2555–67. https://doi.org/10.1002/1097-0258(20000915/30)19:17/18%3C2555::AID-SIM587%3E3.0.CO;2-%23.
23. Richardson S, Thomson A, Best N, Elliott P. Interpreting posterior relative risk estimates in disease-mapping studies. Environ Health Perspect. 2004;112(9):1016–25. https://doi.org/10.1289/ehp.6740.
24. Spiegelhalter DJ, Best NG, Carlin BP, Van Der Linde A. Bayesian measures of model complexity and fit. J R Stat Soc Ser B Stat Methodol. 2002;64(4):583–639. https://doi.org/10.1111/1467-9868.00353.
25. Watanabe S. Asymptotic equivalence of Bayes cross validation and widely applicable information criterion in singular learning theory. J Mach Learn Res. 2010;11:3571–94. Export Date: 22 August 2024; Cited By: 1784.
26. Held L, Schrödle B, Rue H. In: Kneib T, Tutz G, editors. Posterior and Cross-validatory Predictive Checks: A Comparison of MCMC and INLA. Heidelberg: Physica-Verlag HD; 2010. pp. 91–110. https://doi.org/10.1007/978-3-7908-2413-1_6.
27. Gómez-Rubio V. Bayesian Inference with INLA. Boca Raton: Chapman & Hall/CRC Press; 2021.
28. R Core Team. R: A Language and Environment for Statistical Computing. Vienna; 2024. https://www.R-project.org/.
29. Lindgren F, Rue H. Bayesian Spatial Modelling with R-INLA. J Stat Softw. 2015;63(19):1–25.
30. Larosa E, Djuric O, Cassinadri M, Cilloni S, Bisaccia E, Vicentini M, et al. Secondary transmission of COVID-19 in preschool and school settings in northern Italy after their reopening in September 2020: a population-based study. Euro Surveill. 2020;25(49). https://doi.org/10.2807/1560-7917.Es.2020.25.49.2001911.
31. Nikolopoulou GB, Maltezou HC. COVID-19 in Children: Where do we Stand? Arch Med Res. 2022;53(1):1–8. https://doi.org/10.1016/j.arcmed.2021.07.002.
32. Kelly C, White P, Kennedy E, O'Flynn D, Colgan A, Ward M, et al. Limited transmission of SARS-CoV-2 in schools in Ireland during the 2020-2021 school year. Euro Surveill. 2023;28(15). https://doi.org/10.2807/1560-7917.Es.2023.28.15.2200554.
33. Doron S, Ingalls RR, Beauchamp A, Boehm JS, Boucher HW, Chow LH, et al. Weekly SARS-CoV-2 screening of asymptomatic kindergarten to grade 12 students and staff helps inform strategies for safer in-person learning. Cell Rep Med. 2021;2(11): 100452. https://doi.org/10.1016/j.xcrm.2021.100452.
34. Perramon A, Soriano-Arandes A, Pino D, Lazcano U, Andrés C, Català M, et al. Schools as a Framework for COVID-19 Epidemiological Surveillance of Children in Catalonia, Spain: A Population-Based Study. Front Pediatr. 2021;9: 754744. https://doi.org/10.3389/fped.2021.754744.
35. Al-Kuwari MG, Mohammed AM, Abdulmajeed J, Al-Romaihi H, Al-Mass M, Abushaikha SS, et al. COVID-19 testing, incidence, and positivity trends among school age children during the academic years 2020–2022 in the State of Qatar: special focus on using CDC indicators for community transmission to evaluate school attendance policies and public health response. BMC Pediatr. 2024;24(1):374. https://doi.org/10.1186/s12887-024-04833-9.
36. Funk T, Espenhain L, Møller FT, Ethelberg S. Factors associated with the formation of SARS-CoV-2 case-clusters in Danish schools: a nationwide register-based observational study. Epidemiol Infect. 2023;151: e168. https://doi.org/10.1017/s0950268823001188.
37. Colosi E, Bassignana G, Contreras DA, Poirier C, Boëlle PY, Cauchemez S, et al. Screening and vaccination against COVID-19 to minimise school closure: a modelling study. Lancet Infect Dis. 2022;22(7):977–89. https://doi.org/10.1016/s1473-3099(22)00138-4.
38. Maya S, McCorvie R, Jacobson K, Shete PB, Bardach N, Kahn JG. COVID-19 Testing Strategies for K-12 Schools in California: A Cost-Effectiveness Analysis. Int J Environ Res Public Health. 2022;19(15):9371.
39. Yu Z, Bellander T, Bergström A, Dillner J, Eneroth K, Engardt M, et al. Association of Short-term Air Pollution Exposure With SARS-CoV-2 Infection Among Young Adults in Sweden. JAMA Netw Open. 2022;5(4):e228109. https://doi.org/10.1001/jamanetworkopen.2022.8109.
40. Lorenzo JSL, Tam WWS, Seow WJ. Association between air quality, meteorological factors and COVID-19 infection case numbers. Environ Res. 2021;197:111024. https://doi.org/10.1016/j.envres.2021.111024.
41. European Medicines Agency. Comirnaty COVID-19 vaccine: EMA recommends approval for children aged 5 to 11. 2021. https://www.ema.europa.eu/en/news/comirnaty-covid-19-vaccine-ema-recommends-approval-children-aged-5-11. Accessed 18 Dec 2024.
42. Kundi M. Vaccine effectiveness against delta and omicron variants of SARS-CoV-2. BMJ. 2023;381:p1111. https://doi.org/10.1136/bmj.p1111.
43. Viner R, Waddington C, Mytton O, Booy R, Cruz J, Ward J, et al. Transmission of SARS-CoV-2 by children and young people in households and schools: A meta-analysis of population-based and contact-tracing studies. J Infect. 2022;84(3):361–82. https://doi.org/10.1016/j.jinf.2021.12.026.
44. Campagnani G, Bardanzellu F, Pintus MC, Fanos V, Marcialis MA. COVID-19 Vaccination in Children: An Open Question. Curr Pediatr Rev. 2022;18(3):226–36. https://doi.org/10.2174/1573396318666211220093111.
45. Agarwal SK, Naha M. COVID-19 vaccine coverage in India: a district-level analysis. Vaccines (Basel). 2023;11(5). https://doi.org/10.3390/vaccines11050948.
46. Li X, Xu W, Dozier M, He Y, Kirolos A, Lang Z, et al. The role of children in the transmission of SARS-CoV2: updated rapid review. J Glob Health. 2020;10(2):021101. https://doi.org/10.7189/jogh.10.021101.
47. Our World in Data. Weekly confirmed COVID-19 cases per million people. 2024. https://ourworldindata.org/explorers/covid. Accessed 7 Sep 2024.
48. Gharaibeh A, Gharaibeh MA, Bataineh S, Kecerová AM. Exploring the Spatial and Temporal Patterns of Children and Adolescents with COVID-19 Infections in Slovakia during March 2020 to July 2022. Med (Kaunas). 2024;60(6). https://doi.org/10.3390/medicina60060931.
49. Soriano-Arandes A, Brett A, Buonsenso D, Emilsson L, de la Fuente Garcia I, Gkentzi D, et al. Policies on children and schools during the SARS-CoV-2 pandemic in Western Europe. Front Public Health. 2023;11:1175444. https://doi.org/10.3389/fpubh.2023.1175444.
50. Our World in Data. COVID-19 Data Explorer. 2025. https://ourworldindata.org/explorers/covid. Accessed 29 Apr 2025.

Publisher's Note